This is a repository copy of *Doping ruthenium complexes into a molecular spin-crossover material*.

Article:

Doping Ruthenium Complexes into a Molecular Spin-Crossover Material

Laurence J. Kershaw Cook and Malcolm A. Halcrow*

School of Chemistry, University of Leeds, Woodhouse Lane, Leeds LS2 9JT, UK

Tel +44 113 343 6506

Fax +44 113 343 6565

email m.a.halcrow@leeds.ac.uk

Submission for the Special Issue for the 14th International Conference on Molecular Magnetism (ICMM), St Petersburg, Russia

ABSTRACT

Two ruthenium compounds, [Ru(κ^3C,N,C-bip)$_2$][BF$_4$]$_2$ (bip = 2,6-di{1-methylimidazol-2-ylidene-3-yl}pyridine) and [Ru(terpy)(κ^3N,N,C-terpy*)][BF$_4$]$_2$ (terpy = 2,2':6',2"-terpyridine and terpy* = 2,2':6',4"-terpyridine), have been investigated as dopants for the spin-crossover lattice [Fe(bpp)$_2$][BF$_4$]$_2$ (bpp = 2,6-di{pyrazol-1-yl}pyridine). While [Fe(bpp)$_2$][BF$_4$]$_2$ and [Ru(bip)$_2$][BF$_4$]$_2$ did not co-crystallize, five different compositions of solid solutions [Fe(bpp)$_2$]$_x$[Ru(terpy)(terpy*)]$_{1-x}$[BF$_4$]$_2$ were prepared, with $0.96 \geq x \geq 0.13$. The materials with intermediate compositions ($0.58 \geq x \geq 0.28$) contained a mixture of crystalline and amorphous material by powder diffraction. The spin-crossover midpoint temperature ($T_{\frac{1}{2}}$) in [Fe(bpp)$_2$]$_x$[Ru(terpy)(terpy*)]$_{1-x}$[BF$_4$]$_2$ decreases smoothly with x, as the larger ruthenium dopant expands the host lattice and stabilizes its high-spin state. That contrasts with our previously published materials [Fe(bpp)$_2$]$_z$[Ru(terpy)$_2$]$_{1-z}$[BF$_4$]$_2$, which show a more complicated relationship between $T_{\frac{1}{2}}$ and their composition.

INTRODUCTION

The continued world-wide interest in thermally and optically switchable spin-crossover compounds [1-3] reflects their use as switching centers in nanoscience [4], as contrast agents for magnetic resonance imaging [5], as reported groups in solid state and solution-phase sensors [6, 7], and in thermochromic devices [8]. A current challenge is to prepare multifunctional materials, that use spin-crossover switching to modulate another physical property in a bulk material, or at the molecular level [9]. Thus, for example, spin-crossover complexes or hybrid materials exhibiting semiconductor [10], fluorescence [11], magnetic ordering [12] and mesophase functionalities [13] have all been obtained. In some of these cases the effect of spin-crossover on the ancillary property is small, but this remains a promising method for the production of switchable molecule-based materials.

Five years ago we introduced a new approach to this goal, of doping molecular spin-crossover materials with other functional complexes. Our initial work has produced homogeneous solid solutions of $[Fe(bpp)_2][BF_4]_2$ (bpp = 2,6-di{pyrazol-1-yl}pyridine) [14] with $[M(terpy)_2][BF_4]_2$ complexes (terpy = 2,2':6',2''-terpyridine; M = Ru [15, 16], Co [16, 17] or Cu [18]; Scheme 1). This work afforded solid materials exhibiting both spin-crossover with fluorescence, albeit at different temperatures [15], and the first observation of allosteric switching of two different spin-crossover centers in the same material [17]. The $[Fe(bpp)_2][BF_4]_2$ host and $[M(terpy)_2][BF_4]_2$ dopants are particularly suited to each other because they have the same molecular symmetry and charge balance; their cations are similar (but not identical) in size and shape; and, although they are not isostructural, the two compounds adopt the same type of "terpyridine embrace" crystal packing motif [15].

3

[Fe(bpp)₂]²⁺ ... [M(terpy)₂]²⁺ (M = Co, Cu, Ru) ... [Ru(bip)₂]²⁺ ... [Ru(terpy)(terpy*)]²⁺
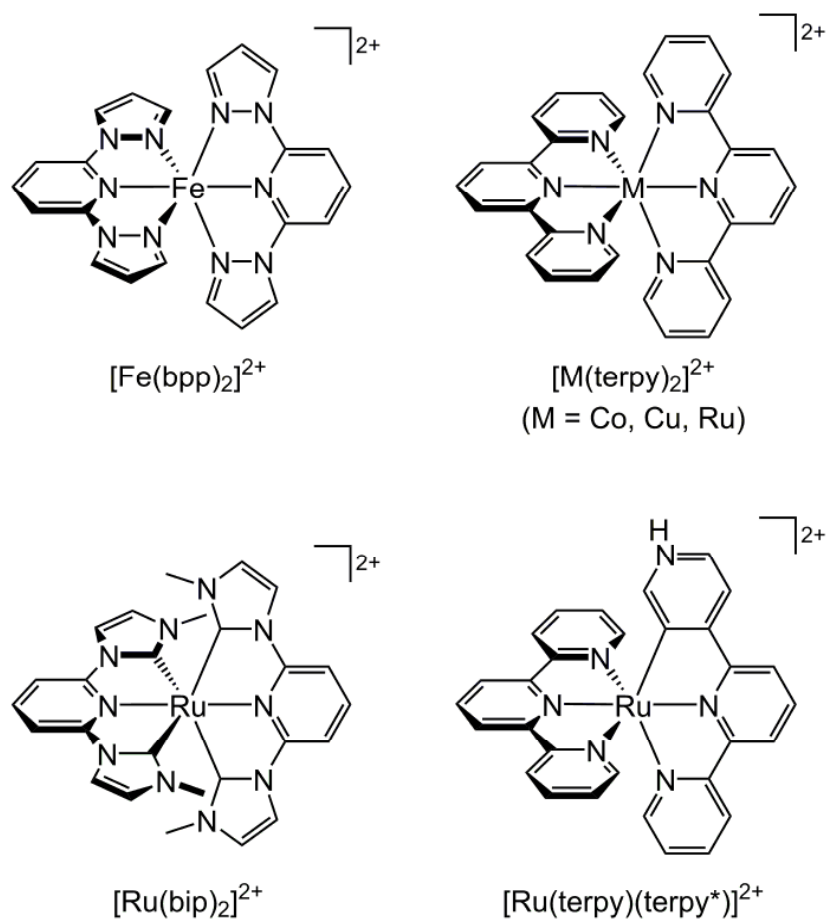
Scheme 1. The compounds referred to in this work.

As a continuation of this work, we were interested to see what other dopant complexes we could incorporate into [Fe(bpp)₂][BF₄]₂. We report here an investigation of two other dopant compounds, [Ru(bip)₂][BF₄]₂ (bip = 2,6-di{1-methylimidazol-2-ylidene-3-yl}pyridine) [19] and [Ru(terpy)(terpy*)][BF₄]₂ (terpy* = 2':6',4"-terpyridine; Scheme 1) [20]. These dopants were selected because they are significantly more emissive than [Ru(terpy)₂]²⁺ at room temperature, which could lead to doped materials showing improved fluorescence properties. In addition, although they have the same symmetry and charge, the shapes of these dopant molecules differ more strongly from [Fe(bpp)₂]²⁺ than the [M(terpy)₂]²⁺ dopants we have used up to now. Hence this study also provides an important test of the flexibility of our dopant approach to multifunctional spin-crossover materials.

4

EXPERIMENTAL

The syntheses of 2,6-di(1'-methylimidazolium-3'-yl)pyridine dibromide ([bipH$_2$]Br$_2$) [19], 2,2':6',4''-terpyridine (terpy*) [20], [RuCl$_3$(terpy)] [21] and [Fe(bpp)$_2$][BF$_4$]$_2$ [15] followed the literature procedures. All other manipulations were carried out in air, using reagent-grade solvents.

Synthesis of [Ru(bip)$_2$][BF$_4$]$_2$

A solution of RuCl$_3$.3H$_2$O (0.10 g, 0.39 mmol) and [bipH$_2$]Br$_2$ (0.31 g. 0.78 mmol) in ethylene glycol (7 cm^3) was held at 190 °C for 4 h. After cooling water was added (10 cm^3), and the solution was then saturated with NaBF$_4$. Stirring for 30 mins yielded a yellow precipitate which was collected, washed in succession with H$_2$O, MeOH and Et$_2$O and dried *in vacuo*. Yield 0.12 g, 41%. Found: C, 40.8; H, 3.40; N, 18.3 %. Calcd for C$_{26}$H$_{26}$B$_2$F$_8$N$_{10}$Ru.H$_2$O: C, 40.5; H, 3.66; N, 18.2 %. ES MS *m/z* 290.1 [Ru(bip)$_2$]$^{2+}$. ^{1}H NMR (CD$_3$NO$_2$) δ 2.74 (s, 12H, C*H*$_3$), 7.02 (d, 2.3 Hz, 4H, Im *H*^{5}), 7.91 (d, 8.3 Hz, 4H, Py *H*$^{3/5}$), 8.04 (d, 2.3 Hz, 4H, Im *H*^{4}), 8.28 (t, 8.1 Hz, 2H, Py *H*^{4}). ^{13}C NMR (CD$_3$NO$_2$) δ 36.4 (4C, *C*H$_3$), 107.0 (4C, Im *C*^{5}), 117.5 (4C, Py *H*$^{3/5}$), 125.4 (4C, Im *C*^{4}), 138.9 (4C, Py *C*^{2}), 153.0 (2C, Py *H*^{4}), 192.0 (4C, Im *C*^{2}). UV/vis (MeCN) λ_{max}, nm (ε_{max}, 10^3 dm^{3}mol^{-1}cm^{-1}) 236 (45.3), 273 (34.9), 280 (sh), 345 (14.1), 383 (19.0), 415 (sh). Fluorescence (MeCN, excitation wavelength 383 nm) λ_{max}^{em} 531 nm.

Synthesis of [Ru(terpy)(terpy*)$_2$][BF$_4$]$_2$

Solid terpy* (0.18 g, 0.78 mmol) was added to a suspension of [RuCl$_3$(terpy)] (0.34 g, 0.78 mmol) in ethylene glycol (15 cm^3) and the mixture was then heated to reflux for 30 mins. After cooling to room temperature the solution was filtered, and saturated aqueous NaBF$_4$ (150 cm^3) was added to the filtrate which resulted in precipitation of the complex which was collected by filtration. The dark purple complex was recrystallized from MeNO$_2$/Et$_2$O. Yield

0.45 g, 77 %. Found: C, 45.2; H, 3.00; N, 11.2 %. Calcd for $C_{30}H_{22}B_2F_8N_6Ru \cdot MeNO_2 \cdot H_2O$: C, 45.4; H, 3.32; N, 10.8. ES MS m/z 284.0 $[Ru(terpy)(terpy^*)]^{2+}$, 567.1 $[Ru(terpy)(terpy^*-H)]^+$. ^1H NMR (CD_3CN) δ 7.05 (s, 1H, $H^{2''}*$), 7.06 (ddd, 1.3, 5.6 and 7.3 Hz, 2H, H^5), 7.17 (ddd, 1.3, 5.2 and 7.3 Hz, 1H, $H^{5}*$), 7.29 (ddd, 0.9, 1.7 and 5.6 Hz, 2H, H^6), 7.52 (ddd, 0.9, 1.7 and 5.2 Hz, 1H, $H^{6}*$), 7.82 (pseudo-td, 1.7 and 7.3 Hz, 2H, H^4), 7.93 (pseudo-td, 1.7 and 7.7 Hz, 1H, $H^{4}*$), 7.95 (dd, 1.3 and 6.0 Hz, 1H, $H^{6''}*$), 8.17 (d, 6.0 Hz, 1H, $H^{5''}*$), 8.22 (t, 8.1 Hz, 1H, H^4), 8.25 (t, 8.1 Hz, 1H, $H^{4'}*$), 8.43 (ddd, J = 0.8, 1.6 and 8.2 Hz, 2H, H^3), 8.51 (ddd, 0.9, 1.2 and 8.3 Hz, 1H, $H^{3}*$), 8.61 (dd, 0.9 and 8.1 Hz, 1H, $H^{5'}*$), 8.65 (d, 8.1 Hz, 2H, $H^{3'/5'}$), 8.67 (dd, 0.9 and 8.1 Hz, 1H, $H^{3'}*$), 13.11 (br s, 1H, NH). ^{13}C NMR (CD_3CN) δ 120.5 (1C, $C^{5''}*$), 124.1 (2C, C^3), 124.5 (1C, $C^{5}*$), 124.8 (1C, $C^{3'}*$), 124.9 (2C, $C^{3'/5'}$), 125.2 (1C, $C^{3}*$), 128.0 (2C, C^5), 128.2 (1C, $C^{5'}*$), 133.3 (2C, C^4), 134.7 (1C, $C^{6''}*$), 136.3 (1C, $C^{4}*$), 137.6 (1C, $C^{4'}$), 139.4 (1C, $C^{4'}*$), 146.3 (1C, $C^{2''}*$), 152.1 (1C, $C^{6'}*$), 152.6 (2C, C^6), 155.2 (2C, C^2), 156.9 and 157.4 (both 1C, $C^{2}*$ and $C^{2'}*$), 158.4 (2C, $C^{2'/6'}$), 160.9 (1C, $C^{6}*$), 167.0 (1C, $C^{4'}*$), 182.4 (1C). UV/vis (MeCN) λ_{max}, nm (ε_{max}, 10^3 $dm^3mol^{-1}cm^{-1}$) 235 (31.9), 274 (27.0), 312 (33.2), 360 (4.8), 435 (sh), 509 (8.3). Fluorescence (MeCN, excitation wavelength 354 nm) λ_{max}^{em} 783 nm.

Synthesis of the solid solutions

The appropriate mole ratios of $[Fe(bpp)_2][BF_4]_2$ (98 mg, 0.15 mmol) and $[Ru(terpy)(terpy^*)_2][BF_4]_2$ were dissolved in $MeNO_2$ (5 cm^3), and filtered. Diffusion of diethyl ether vapor into the filtered solutions afforded microcrystalline materials which were collected by filtration, washed with diethyl ether and dried *in vacuo*. Crystallized yields ranged from 55-77 %.

$x = 0.96$: $[Fe(bpp)_2][BF_4]_2$ (98 mg, 0.15 mmol) and $[Ru(terpy)(terpy^*)_2][BF_4]_2$ (12 mg, 0.02 mmol) yielded a purple red-powder. Found: C, 40.8; H, 2.80; N, 21.0 %. Calcd for $[C_{22}H_{18}B_2F_8FeN_{10}]_{0.96}[C_{30}H_{22}B_2F_8N_6Ru]_{0.04}$ C, 40.9; H, 2.79; N, 21.0 %.

$x = 0.85$: [Fe(bpp)$_2$][BF$_4$]$_2$ (78 mg, 0.12 mmol) and [Ru(terpy)(terpy*)$_2$][BF$_4$]$_2$ (30 mg, 0.04 mmol) yielded a dark powder. Found: C, 41.6; H, 2.90; N, 19.5 %. Calcd for [C$_{22}$H$_{18}$B$_2$F$_8$FeN$_{10}$]$_{0.85}$[C$_{30}$H$_{22}$B$_2$F$_8$N$_6$Ru]$_{0.15}$ C, 41.9; H, 2.81; N, 19.8 %.

$x = 0.58$: [Fe(bpp)$_2$][BF$_4$]$_2$ (52 mg, 0.08 mmol) and [Ru(terpy)(terpy*)$_2$][BF$_4$]$_2$ (59 mg, 0.08 mmol) gave a dark microcrystalline solid. Found: C, 42.9; H, 2.95; N, 16.4 %. Calcd for [C$_{22}$H$_{18}$B$_2$F$_8$FeN$_{10}$]$_{0.58}$[C$_{30}$H$_{22}$B$_2$F$_8$N$_6$Ru]$_{0.42}$·H$_2$O C, 43.1; H, 3.09; N, 16.5 %.

$x = 0.28$: [Fe(bpp)$_2$][BF$_4$]$_2$ (26 mg, 0.04 mmol) and [Ru(terpy)(terpy*)$_2$][BF$_4$]$_2$ (88 mg, 0.12 mmol) yielded a dark polycrystalline material. Found: C, 45.2; H, 3.10; N, 13.3 %. Calcd for [C$_{22}$H$_{18}$B$_2$F$_8$FeN$_{10}$]$_{0.28}$[C$_{30}$H$_{22}$B$_2$F$_8$N$_6$Ru]$_{0.72}$·H$_2$O C, 45.4; H, 3.14; N, 13.6 %.

$x = 0.13$: [Fe(bpp)$_2$][BF$_4$]$_2$ (8 mg, 0.01 mmol) and [Ru(terpy)(terpy*)$_2$][BF$_4$]$_2$ (84 mg, 0.11 mmol) yielded large dark purple crystals. Found: C, 45.7; H, 3.15; N, 12.1 %. Calcd for [C$_{22}$H$_{18}$B$_2$F$_8$FeN$_{10}$]$_{0.13}$[C$_{30}$H$_{22}$B$_2$F$_8$N$_6$Ru]$_{0.87}$·2H$_2$O C, 45.4; H, 3.35; N, 11.9 %.

Single crystal X-ray structure determination

Single crystals of formula [Ru(bip)$_2$][BF$_4$]$_2$·0.75CH$_3$NO$_2$ were obtained by slow diffusion of diethyl ether vapor into a nitromethane solution of the complex. Experimental details of the structure determination are given in Table 1. The crystals have a high mosaicity, which accounts for the high R_{int} and R_1 parameters in the table and the low precision of the refinement. Diffraction data were collected with an Agilent Supernova dual-source diffractometer using monochromated Mo-K_α radiation radiation ($\lambda = 0.71073$ Å). The diffractometer is fitted with Oxford Cryostream low-temperature devices. The structure was solved by direct methods *(SHELXS97* [22]), and developed by full least-squares refinement on F^2 (*SHELXL97* [22]). Crystallographic figures were prepared using *XSEED* [23].

The asymmetric unit contains two half-molecules of the complex dication, with Ru(1) lying on the C_2 axis 0, y, ¼ and Ru(20), N(21), C(24), N(31) and N(34) all lying on the C_2 axis ½, y, ¼. There are also two BF_4^- ions lying on general crystallographic sites, and a nitromethane molecule that was modelled over two orientations with occupancies 0.5 and 0.25. The fixed restraints C−N = 1.45(2), N−O = 1.22(2), O...O = 2.09(2) and C...O = 2.30(2) Å were applied to the solvent molecules. All non-H atoms except the minor partial solvent residue were refined anisotropically, and H atoms were placed in calculated positions and refined using a riding model. Large displacement ellipsoids on C(23) and C(24) probably reflect librational disorder in that pyridyl ring, caused by a short intermolecular contact to the disordered solvent site [C(23)...C(51B^i) = 3.08 Å; symmetry code (i) = ½+x, ½+y, z]. Attempts to refine that ligand disorder did not afford a sensible model, however, and did not significantly improve the residuals.

Other measurements.

Electrospray mass spectra were obtained using a Waters Micromass LCT TOF spectrometer, in a MeOH matrix. CHN microanalyses were performed by the University of Leeds Department of Chemistry microanalytical service. Magnetic susceptibility measurements were obtained using a Quantum Design SQUID/VSM magnetometer, in an applied field of 1000 G and a temperature ramp of 2 Kmin^{-1}. Diamagnetic corrections were estimated from Pascal's constants [24]. X-ray powder diffraction measurements used a Bruker D8 Advance A25 diffractometer, using Cu-K_α radiation (λ = 1.5418 Å). Thermogravimetric analyses employed a TA Instruments TGA 2050 analyser.

Table 1. Experimental details for the single crystal structure determination of [Ru(bip)$_2$][BF$_4$]$_2$·0.75CH$_3$NO$_2$.

Formula	C$_{26.75}$H$_{28.25}$B$_2$F$_8$N$_{10.75}$O$_{1.50}$Ru
M_r	799.04
Crystal system	monoclinic
Space Group	$C2/c$
a (Å)	17.1318(14)
b (Å)	21.361(2)
c (Å)	18.508(2)
β (°)	99.124(9)
V (Å^3)	6687.6(11)
Z	8
D_{calc} (g.cm^{-3})	1.587
μ (Mo-K_α, mm^{-1})	0.556
T (K)	100(2)
Measured reflections	15014
Independent reflections	7491
R_{int}	0.104
Observed reflections [$I > 2\sigma(I)$]	4088
Data, restraints, parameters	7491, 12, 483
$R_1(I > 2\sigma(I))^a$, wR_2(all data)^b	0.091, 0.180
GOF	1.041
$\Delta\rho_{min}$, $\Delta\rho_{max}$ (e.Å^{-3})	−0.95, 0.85

$^a R = \Sigma\,[\,|F_o| - |F_c|\,]\,/\,\Sigma\,|F_o|$ $\qquad$ $^b wR = [\Sigma w(F_o^2 - F_c^2)\,/\,\Sigma wF_o^4]^{1/2}$

RESULTS AND DISCUSSION

The dopant complexes [Ru(bip)$_2$]$^{2+}$ and [Ru(terpy)(terpy*)]$^{2+}$ have both been previously

prepared, as salts with PF$_6{}^-$ or BPh$_4{}^-$ counterions [19, 20]. We needed the BF$_4{}^-$ salts of the

compounds in this work, for compatibility with the [Fe(bpp)$_2$][BF$_4$]$_2$ host lattice. Both

[Ru(bip)$_2$][BF$_4$]$_2$ and [Ru(terpy)(terpy*)][BF$_4$]$_2$ were prepared by the same literature

procedures, but using excess aqueous NaBF$_4$ to precipitate the final products. Both

compounds retained solvent or atmospheric moisture in the solid state by microanalysis. A

single crystal X-ray structure of [Ru(bip)$_2$][BF$_4$]$_2$·0.75CH$_3$NO$_2$ confirmed the presence of

lattice solvent, and showed that the compound does not adopt the same "terpyridine embrace" crystal packing [25] adopted by [Fe(bpp)$_2$][BF$_4$]$_2$ and [Ru(terpy)$_2$][BF$_4$]$_2$. That might make it a less compatible dopant for [Fe(bpp)$_2$][BF$_4$]$_2$, based on our previous arguments [15]. Although the precision of the refinement is low, the molecular geometry of the [Ru(bip)$_2$]$^{2+}$ complex is similar to other ruthenium complexes of this class of *bis*-carbenyl chelate ligand (Fig. 1) [19, 26]. The Ru−N bond lengths range from 2.010(8)-2.020(6) Å, while the Ru−C distances are 2.035(8)-2.045(8) Å. Single crystals of [Ru(terpy)(terpy*)][BF$_4$]$_2$ were not obtained, but the solid compound contains a mixture of amorphous and crystalline material by X-ray powder diffraction, and is not isostructural with [Ru(terpy)$_2$][BF$_4$]$_2$ (see below).

As a preliminary test to rule out ligand exchange between the iron and ruthenium centers during their co-crystallization, solutions of [Fe(bpp)$_2$][BF$_4$]$_2$ and either [Ru(bip)$_2$][BF$_4$]$_2$ or [Ru(terpy)(terpy*)][BF$_4$]$_2$ in CD$_3$NO$_2$ were analysed by ^{1}H NMR at daily intervals. No change in the spectra was observed over three days, which is the typical time required for these compounds to crystallize. After *ca.* 5 days the spectra began to broaden however, with weak new resonances appearing in the diamagnetic region (Fig. 2). It is unclear whether this reflects exchange of tridentate ligands between the iron and ruthenium ions, or simply decomposition of the organometallic ruthenium complexes (some precipitation of the intact [Ru(terpy)(terpy*)][BF$_4$]$_2$ occurred after *ca.* 1 week, which may be a contributing factor to those spectral changes). None-the-less, it is clear that the host compound and the two dopant complexes retain their integrity during the 1-2 days required for the synthesis of the solid solutions described below.
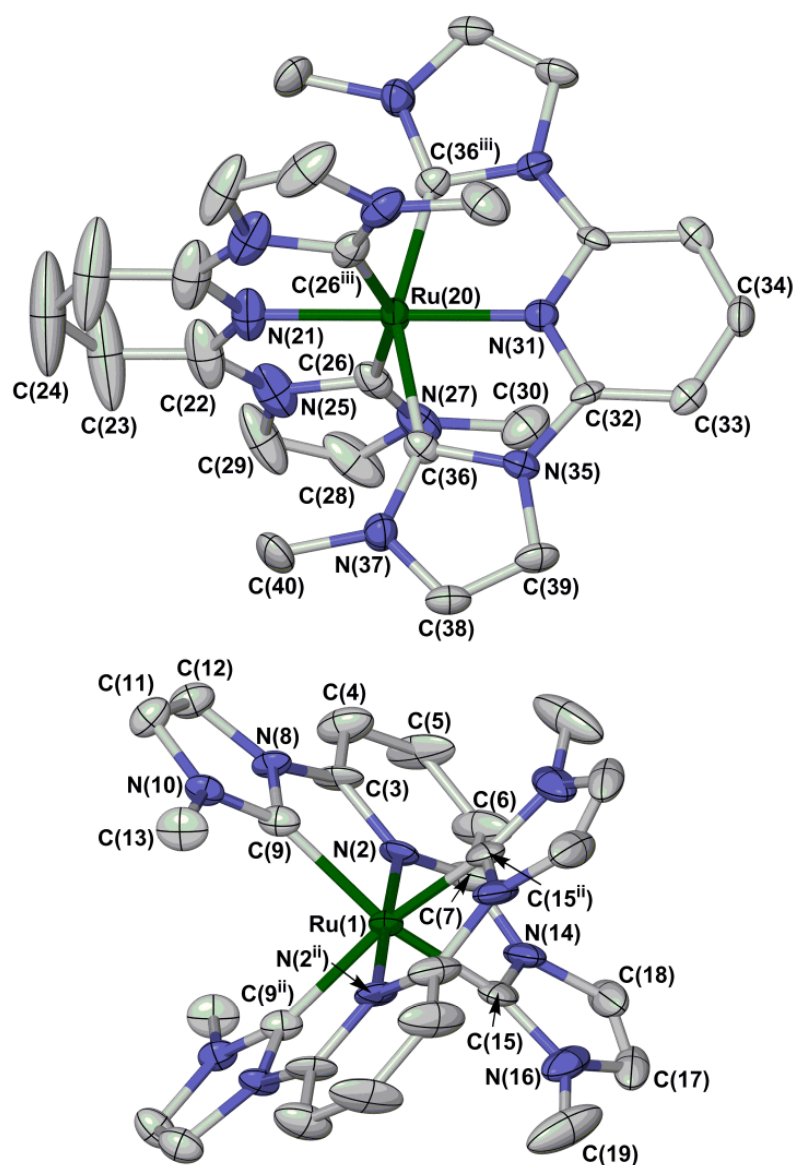
Figure 1 The two unique complex molecules in the crystal structure of [Ru(bip)$_2$][BF$_4$]$_2$·0.75CH$_3$NO$_2$. Displacement ellipsoids are at the 50 % probability level, and H atoms are omitted for clarity. The large displacement ellipsoids on C(23) and C(24) reflect librational disorder, caused by a close intermolecular C…C contact to the disordered solvent. Symmetry codes: (ii) –x, y, ½–z; (iii) 1–x, y, ½–z.
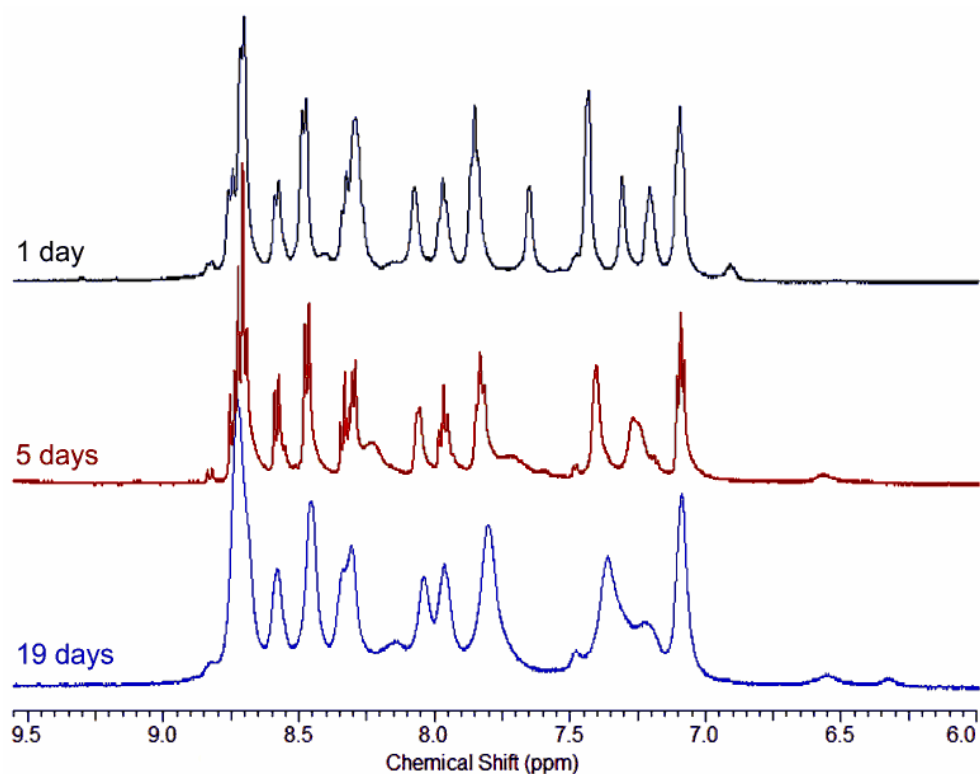
Figure 2 The diamagnetic, aromatic region of the ^{1}H NMR spectra of a 1:1 mixture of [Fe(bpp)$_2$][BF$_4$]$_2$ and [Ru(terpy)(terpy*)][BF$_4$]$_2$ in CD$_3$NO$_2$ at 293 K. The spectra were run 1 day (top), 5 days (center) and 19 days (bottom) after mixing the complexes.

Following our previous protocol [15, 17, 18], nitromethane solutions containing [Fe(bpp)$_2$][BF$_4$]$_2$ and either of the two dopants in pre-defined mole ratios were recrystallized by slow diffusion of diethyl ether antisolvent at room temperature, over a period of 1-2 days. When [Ru(bip)$_2$][BF$_4$]$_2$ was used as the dopant, the resultant polycrystalline solid was clearly heterogeneous, containing two types of crystal which were manually separated, and identified as pure [Fe(bpp)$_2$][BF$_4$]$_2$ and [Ru(bip)$_2$][BF$_4$]$_2$ by ^{1}H NMR. Therefore, solid solutions of these complexes do not form under these conditions, and [Ru(bip)$_2$][BF$_4$]$_2$ was not investigated further as a dopant. However, material obtained from co-crystallization of

12

[Fe(bpp)$_2$][BF$_4$]$_2$ and [Ru(terpy)(terpy*)][BF$_4$]$_2$ was visually homogeneous, and was therefore investigated further. Five different compositions were prepared of formula [Fe(bpp)$_2$]$_x$[Ru(terpy)(terpy*)]$_{1-x}$[BF$_4$]$_2$·yH$_2$O, with x = 0.96, 0.85, 0.58, 0.28 and 0.13. In contrast to our previous work [15-18], x was consistently higher by microanalysis than expected from the mole ratios of the complexes in the crystallization solutions. That may reflect a higher solubility of the ruthenium dopant compared to the iron complex, which therefore crystallizes preferentially. The water content of the materials (y) is 0 when x is large but increases at higher concentrations of the ruthenium complex (which also contains lattice solvent in its pure form). The presence of this lattice water in the solid solutions was confirmed by TGA analyses (Fig. 3).
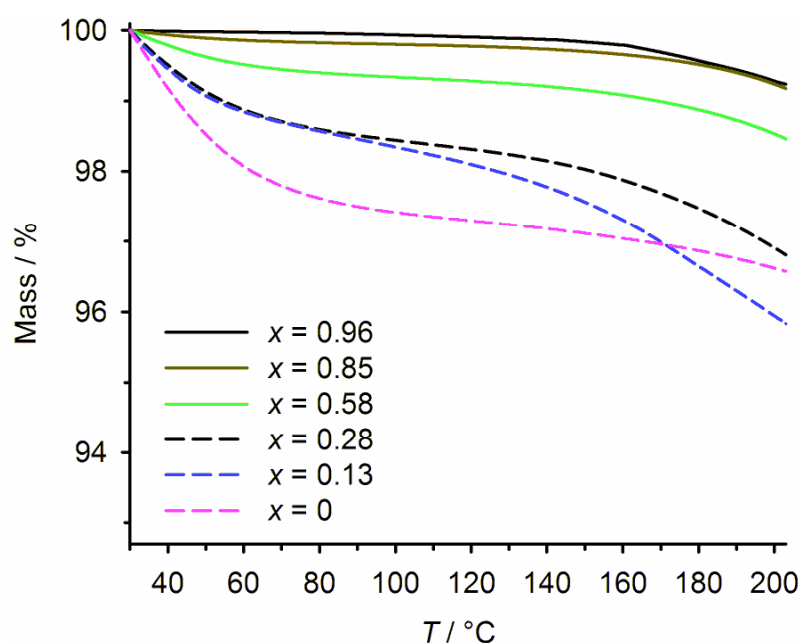

Figure 3 Thermogravimetric analyses of [Fe(bpp)$_2$]$_x$[Ru(terpy)(terpy*)]$_{1-x}$[BF$_4$]$_2$·yH$_2$O, showing the increased presence of lattice solvent (y) with increasing ruthenium content. Loss of 1 equiv H$_2$O corresponds to *ca.* 2 % mass loss, depending on the sample.

X-ray powder diffraction showed that the solid solutions with $x = 0.96$ and 0.85 were homogeneous, crystalline and isostructural with pure $[Fe(bpp)_2][BF_4]_2$ (Fig. 4). Conversely the ruthenium-rich material with $x = 0.13$ is also phase pure, and isostructural with the pure ruthenium complex. However, the two intermediate compositions were less crystalline and contain a mixture of both crystal phases and some amorphous material, with the $[Fe(bpp)_2][BF_4]_2$ phase predominating when $x = 0.58$ and the $[Ru(terpy)(terpy^*)][BF_4]_2$ structure being in the majority when $x = 0.28$ (Fig. 4). This is comparable to the $[Fe(bpp)_2]_z[Ru(terpy)_2]_{1-z}[BF_4]_2$ system where mixed-phase materials were obtained for $0.75 \geq z \geq 0.28$, although the intermediate compositions in that system were more crystalline than in this work by powder diffraction [15].

Pure $[Fe(bpp)_2][BF_4]_2$ exhibits an abrupt spin-transition at 260 K, with a small hysteresis loop ($\Delta T = $ 2-3 K [14, 15]). Spin-crossover in $[Fe(bpp)_2]_x[Ru(terpy)(terpy^*)]_{1-x}[BF_4]_2 \cdot yH_2O$ follows two consistent trends, according to magnetic susceptibility data (Fig. 5 and Table 2). First, the transition midpoint temperature $T_{\frac{1}{2}}$ gradually decreases with increasing mole fraction of ruthenium. That is the expected trend, since the dopant molecule is larger than the iron complex, which is in turn larger in its high-spin state. Thus, a higher dopant concentration expands the crystal lattice [16] and stabilizes the high-spin state of the host material [27]. Second, the transition becomes less cooperative as x decreases. When $x \geq 0.85$ this manifests as a narrowing of the transition hysteresis, but at higher dopant concentrations the transition broadens considerably, to the extent that no defined spin-crossover event is detectable for $x = 0.13$ (Fig. 5). That is again typical behavior for spin-crossover materials containing inert dopants, which disrupt the elastic interactions between the iron centers in the solid lattice [28]. Moreover, the abrupt spin-transitions in these solid solutions are superimposed upon an underlying, more gradual spin-crossover equilibrium which becomes more pronounced as x decreases (Fig. 5). We attribute this behavior to the mixed

14
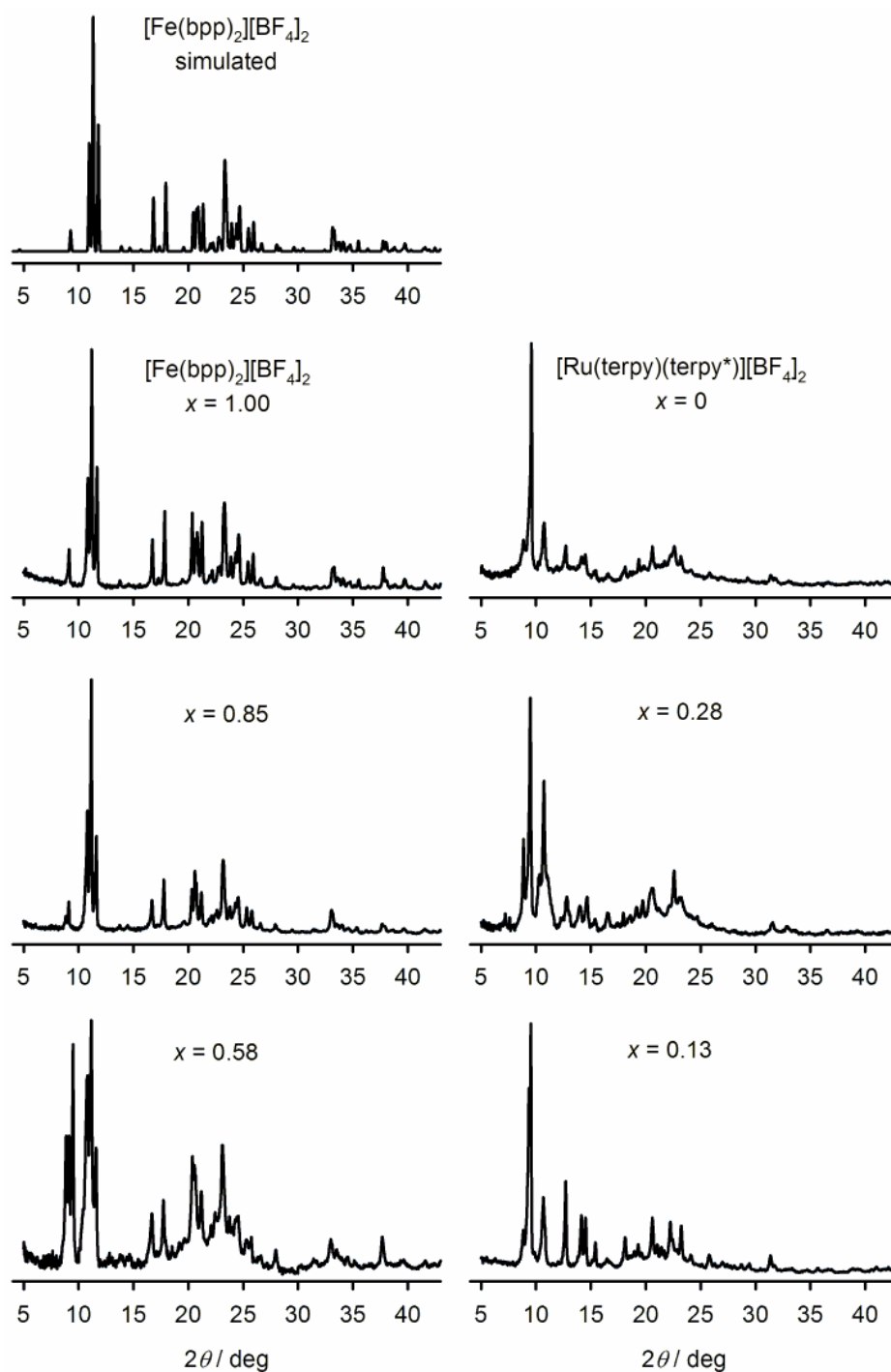
Figure 4 X-ray powder diffraction data for different compositions of solid solution [Fe(bpp)$_2$]$_x$[Ru(terpy)(terpy*)]$_{1-x}$[BF$_4$]$_2$ at 298 K. A simulation derived from the crystal structure of the pure [Fe(bpp)$_2$][BF$_4$]$_2$ phase is also given [15]. The data for $x = 0.96$ are not shown in the Figure, but closely resemble the pattern for $x = 0.85$.
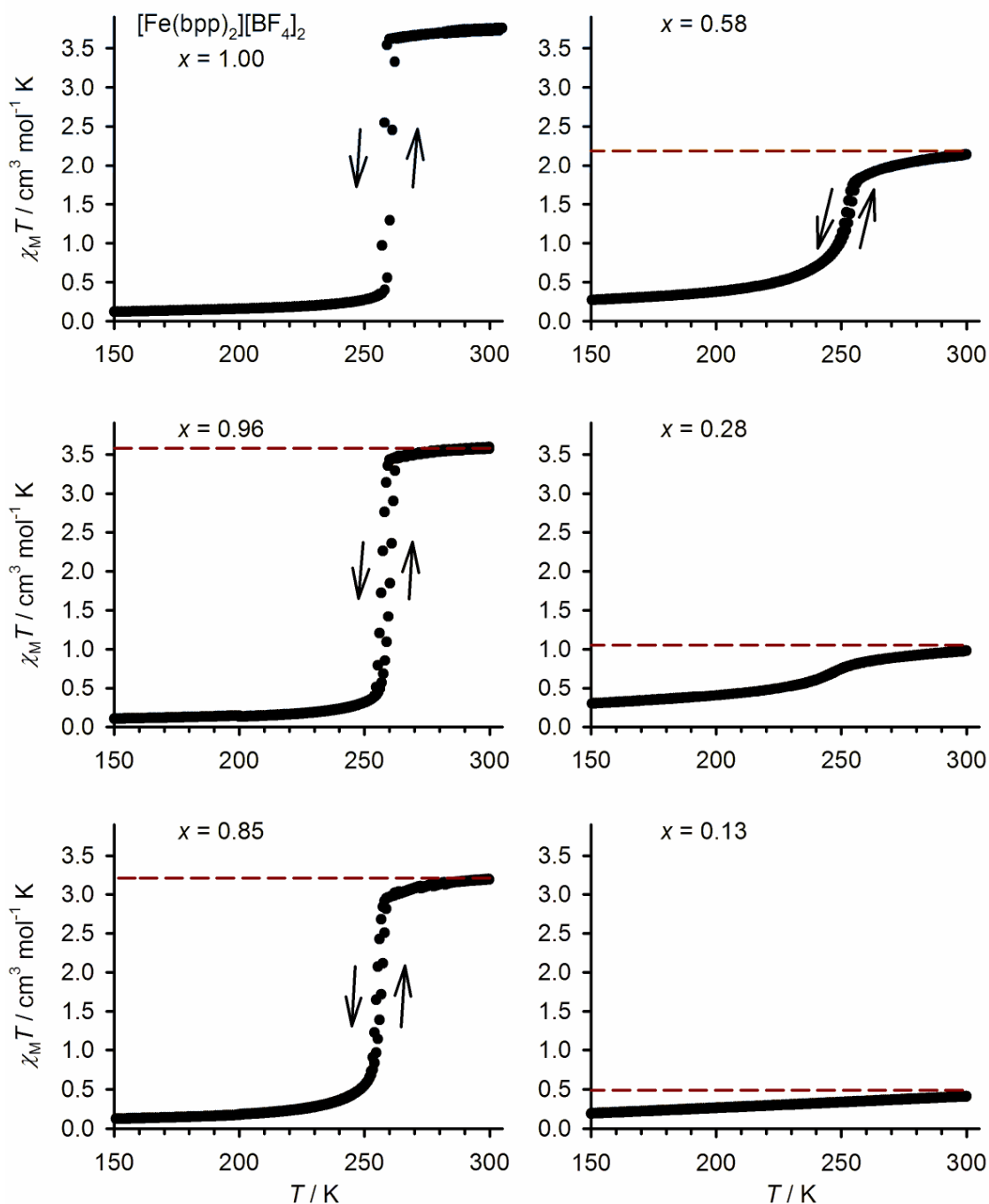
Figure 5 Variable temperature magnetic susceptibility data for different compositions of solid solution $[Fe(bpp)_2]_x[Ru(terpy)(terpy^*)]_{1-x}[BF_4]_2$. All data were measured with coling and warming temperature ramps. The dashed lines show the predicted $\chi_M T$ value for each sample in its fully high-spin state, based on its microanalytical composition. Data for $[Fe(bpp)_2][BF_4]_2$ are taken from ref. [14].

Table 2. Spin-crossover parameters for the $[Fe(bpp)_2]_x[Ru(terpy)(terpy^*)]_{1-x}[BF_4]_2 \cdot yH_2O$
solid solutions. No spin-transition is detectable when $x = 0.13$ (Fig. 3).

x	$T_{1/2}\downarrow$ (K)	$T_{1/2}\uparrow$ (K)	$\Delta T_{1/2}$ (K)
1.00	258	261	3
0.96	257	260	3
0.85	255	256	1
0.58	253	254	1
0.28	251	251	−
0.13	−	−	−

crystalline:amorphous nature of these solid solutions, which is evident by powder diffraction (Fig. 4). Iron centers in the amorphous material would be expected to undergo less cooperative spin-crossover than in a crystalline phase, as observed. Notably co-existing abrupt and gradual spin-transitions were not apparent in our earlier systems $[Fe(bpp)_2]_z[M(terpy)_2]_{1-z}[BF_4]_2$ (M = Ru, Co), which are also fully crystalline by powder diffraction [15, 17].

The relationship between composition and $T_{1/2}$ shows some differences between $[Fe(bpp)_2]_x[Ru(terpy)(terpy^*)]_{1-x}[BF_4]_2 \cdot yH_2O$ and $[Fe(bpp)_2]_z[Ru(terpy)_2]_{1-z}[BF_4]_2$, however. At low dopant concentrations ($x, z \geq 0.75$) the two sets of compounds behave similarly, in that $T_{1/2}$ decreases with increasing dopant at a similar rate (Fig. 6). However, $T_{1/2}$ in $[Fe(bpp)_2]_z[Ru(terpy)_2]_{1-z}[BF_4]_2$ begins to increase when $z < 0.75$, which is also the composition where the materials begin to contain a mixture of crystal phases (Fig. 6) [15]. Hence, $[Fe(bpp)_2]^{2+}$ doped into $[Ru(terpy)_2][BF_4]_2$ exhibits a higher $T_{1/2}$ than in its pure form; that is, the $[Ru(terpy)_2][BF_4]_2$ lattice stabilizes the low-spin state of a $[Fe(bpp)_2]^{2+}$ center to a greater extent than its native $[Fe(bpp)_2][BF_4]_2$ structure [15]. Clearly $[Fe(bpp)_2]^{2+}$ doped into $[Ru(terpy)(terpy^*)][BF_4]_2$ does not behave the same way, and the $[Fe(bpp)_2]_x[Ru(terpy)(terpy^*)]_{1-x}[BF_4]_2 \cdot yH_2O$ materials show a continuous decrease in $T_{1/2}$ with x over the entire composition range.
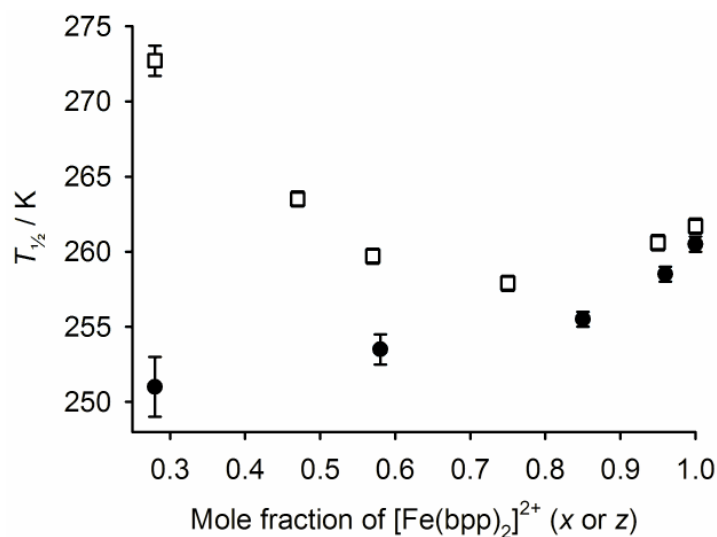
**Figure 6** Variation in spin-crossover midpoint temperature $T_{1/2}$ with composition for

[Fe(bpp)$_2$]$_x$[Ru(terpy)(terpy*)]$_{1-x}$[BF$_4$]$_2$ (●) and [Fe(bpp)$_2$]$_z$[Ru(terpy)$_2$]$_{1-z}$[BF$_4$]$_2$ (□) [15].

The absorption and emission spectra of the ruthenium compounds in this work resemble the

previous reports of those complexes [19,20]. In particular, both the dopant compounds

fluoresce intensely in MeCN solution at room temperature with emission maxima at 531 nm

([Ru(bip)$_2$][BF$_4$]$_2$) and 783 nm ([Ru(terpy)(terpy*)][BF$_4$]$_2$). Neither compound showed an

observable emission in the solid state upon irradiation at 254 or 365 nm at 298 K, however.

The [Fe(bpp)$_2$]$_x$[Ru(terpy)(terpy*)]$_{1-x}$[BF$_4$]$_2$·yH$_2$O solid solutions similarly did not fluoresce

at room temperature.

CONCLUSION

This work has demonstrated both flexibility and limitations to our dopant approach to

multifunctional spin-crossover materials. On one hand, [Fe(bpp)$_2$][BF$_4$]$_2$ and

[Ru(terpy)(terpy*)][BF$_4$]$_2$ were successfully co-crystallized, despite there being no apparent

relationship between the structures of the pure solids by X-ray powder diffraction. The

hydrogen bonding capability of the [Ru(terpy)(terpy*)]$^{2+}$ complex, which has an N−H group

at the periphery of the (formally zwitterionic) terpy* ligand, also has no bearing on its ability to intercalate into the $[Fe(bpp)_2][BF_4]_2$ lattice. In contrast, we observed no evidence for the co-crystallization of $[Fe(bpp)_2][BF_4]_2$ and $[Ru(bip)_2][BF_4]_2$, despite the closer similarity between the shapes of their heterocyclic ligand backbones. That may reflect the methyl substituents on the bip ligands, which could sterically hinder the formation of $\pi...\pi$ interactions between $[Ru(bip)_2]^{2+}$ and nearest neighbor $[Fe(bpp)_2]^{2+}$ molecules. Such interactions are an important component of the terpyridine embrace lattice type adopted by the iron compound [25]. In summary, the most important factor determining whether a dopant complex is suitable for intercalation into $[Fe(bpp)_2][BF_4]_2$ appears to be the shape of the dopant molecule.

SUPPLEMENTARY DATA

CCDC 1010801 contains the supplementary crystallographic data for $[Ru(bip)_2][BF_4]_2 \cdot 0.75CH_3NO_2$. These data can be obtained free of charge via http://www.ccdc.cam.ac.uk/conts/retrieving.html, or from the Cambridge Crystallographic Data Centre, 12 Union Road, Cambridge CB2 1EZ, UK; fax: (+44) 1223-336-033; or e-mail: deposit@ccdc.cam.ac.uk.

REFERENCES

[1]   P. Gütlich, H. A. Goodwin (Eds.) Spin Crossover in Transition Metal Compounds I-III. Top. Curr. Chem. vols. 233-235, Springer Verlag, Berlin, Germany (2004).

[2]   M. A. Halcrow (Ed.) Spin-crossover materials - properties and applications, John Wiley & Sons, Chichester, UK (2013).

[3]   a) P. Gütlich, Eur. J. Inorg. Chem. (2013) 581;

b) P. Gütlich, A. B. Gaspar, Y. Garcia, Beilstein J. Org. Chem. 9 (2013) 342.

[4]   a) A. Bousseksou, G. Molnár, L. Salmon, W. Nicolazzi, Chem. Soc. Rev. 40 (2011) 3313;

b) M. Cavallini, Phys. Chem. Chem. Phys. 14 (2012) 11867.

[5]   J. Hasserodt, J. L. Kolanowski, F. Touti, Angew. Chem. Int. Ed. 53 (2014) 60.

[6]   a) J. Linares, E. Codjovi, Y. Garcia, Sensors 12 (2012) 4479;

b) O. S. Wenger, Chem. Rev. 113 (2013) 3686.

[7]   a) Z. Ni, M. P. Shores, J. Am. Chem. Soc. 131 (2009) 32;

b) M. C. Young, E. Liew, R. J. Hooley, Chem. Commun. 50 (2014) 5043.

[8]   O. Kahn, C. J. Martinez, Science, 279 (1998) 44.

[9]   A. B. Gaspar, V. Ksenofontov, M. Seredyuk, P. Gütlich, Coord. Chem. Rev. 249 (2005) 2661.

[10] a) C. Faulmann, K. Jacob, S. Dorbes, S. Lampert, I. Malfant, M.-L. Doublet, L. Valade, J. A. Real, Inorg. Chem. 46 (2007) 8548;

b) K. Takahashi, H.-B. Cui, Y. Okano, H. Kobayashi, H. Mori, H. Tajima, Y. Einaga, O. Sato, J. Am. Chem. Soc. 130 (2008) 6688;

c) M. Nihei, N. Takahashi, H. Nishikawa, H. Oshio, Dalton Trans. 40 (2011) 2154;

d) W. Xue, B.-Y. Wang, J. Zhu, W.-X. Zhang, Y.-B. Zhang, H.-X. Zhao, X.-M. Chen, Chem. Commun. 47 (2011) 10233;

e) K. Fukuroi, K. Takahashi, T. Mochida, T. Sakurai, H. Ohta, T. Yamamoto, Y. Einaga, H. Mori, Angew. Chem. Int. Ed. 53 (2014) 1983.

[11] a) M. Matsuda, H. Isozaki, H. Tajima, Chem. Lett. 37 (2008) 374;

b) L. Salmon, G. Molnár, D. Zitouni, C. Quintero, C. Bergaud, J.-C. Micheaud, A. Bousseksou, J. Mater. Chem. 20 (2010) 5499;

c) Y. Garcia, F. Robert, A. D. Naik, G. Zhou, B. Tinant, K. Robeyns, S. Michotte, L. Piraux, J. Am. Chem. Soc. 133 (2011) 15850;

d) S. Titos-Padilla, J. M. Herrera, X. W. Chen, J. J. Delgado, E. Colacio, Angew. Chem. Int. Ed. 50 (2011) 3290;

e) R. González-Prieto, B. Fleury, F. Schramm, G. Zoppellaro, R. Chandrasekar, O. Fuhr, S. Lebedkin, M. Kappes, M. Ruben, Dalton Trans. 40 (2011) 7564.

21

[12] a) M. Clemente-León, E. Coronado, C. Martí-Gastaldo, F. M. Romero, Chem. Soc. Rev. 40 (2011) 473;

b) J. H. Yoon, D. W. Ryu, S. Y. Choi, H. C. Kim, E. K. Koh, J. Tao, C. S. Hong, Chem. Commun. 47 (2011) 10416;

c) O. Roubeau, M. Evangelisti, E. Natividad, Chem. Commun. 48 (2012) 7604;

d) E. Coronado, M. Giménez-Marqués, C. Martí-Gastaldo, G. M. Espallargas, E. Navarro-Moratalla, J. C. Waerenborgh, Inorg. Chem. 52 (2013) 8451.

[13] a) S. Hayami, M. R. Karim, Y. H. Lee, Eur. J. Inorg. Chem. (2013) 683;

b) A. B. Gaspar, M. Seredyuk, Coord. Chem. Rev. 268 (2014) 41.

[14] a) J. M. Holland, J. A. McAllister, Z. Lu, C. A. Kilner, M. Thornton-Pett, M. A. Halcrow, Chem. Commun. (2001) 577;

b) J. M. Holland, J. A. McAllister, C. A. Kilner, M. Thornton-Pett, A. J. Bridgeman, M. A. Halcrow, J. Chem. Soc. Dalton Trans. (2002) 548.

[15] C. A. Tovee, C. A. Kilner, J. A. Thomas, M. A. Halcrow, CrystEngComm 11 (2009) 2069.

[16] G. Chastanet, C.A. Tovee, G. Hyett, M. A. Halcrow, J.-F. Létard, Dalton Trans. 41 (2012) 4896.

[17] M. A. Halcrow, Chem. Commun. 46 (2010) 4761.

[18] R. Docherty, F. Tuna, C. A. Kilner, E. J. L. McInnes, M. A. Halcrow, Chem. Commun. 48 (2012) 4055.

[19] S. U. Son, K. H. Park, Y.-S. Lee, B. Y. Kim, C. H. Choi, M. S. Lah, Y. H. Jang, D.-J. Jang, Y. K. Chung, Inorg. Chem. 43 (2004) 6896.

[20] E. C. Constable, A. M. W. Cargill Thompson, J. Cherryman, T. Liddiment, Inorg. Chim. Acta, 235 (1995) 165.

[21] E. C. Constable, A. M. W. Cargill Thompson, D. A. Tocher, M. A. M. Daniels, New J. Chem. 16 (1992) 855.

[22] G. M. Sheldrick, Acta Cryst. Sect. A 64 (2008) 112.

[23] L. J. Barbour, J. Supramol. Chem. 1 (2001) 189.

[24] C. J. O'Connor, Prog. Inorg. Chem. 29 (1982) 203.

[25] J. McMurtrie, I. Dance, CrystEngComm 7 (2005) 216.

[26] a) H.-J. Park, K. H. Kim, S. Y. Choi, H.-M. Kim, W. I. Lee, Y. K. Kang, Y. K. Chung, Inorg. Chem. 49 (2010) 7340;

b) H.-J. Park, Y. K. Chung, Dalton Trans. 41 (2012) 5678.

24

[27] A. Hauser, N. Amstutz, S. Delahaye, A. Sadki, S. Schenker, R. Sieber, M. Zerara, Struct. Bonding 106 (2004) 81.

[28] J. Pavlik, R. Boča, Eur. J. Inorg. Chem. (2013) 697.